Mechanistic simulations predict that thermal and hydrological effects of climate change on Mediterranean trout cannot be offset by adaptive behaviour, evolution, and increased food production

Daniel Ayllón [a,*], Steven F. Railsback [b], Bret C. Harvey [c], Inmaculada García Quirós [d], Graciela G. Nicola [e], Benigno Elvira [a], Ana Almodóvar [a]

[a] Complutense University of Madrid, Faculty of Biology, Department of Biodiversity, Ecology and Evolution, Madrid, Spain
[b] Lang Railsback & Associates, Arcata, CA, USA
[c] Pacific Southwest Research Station, USDA Forest Service, Arcata, CA, USA
[d] Helmholtz Centre for Environmental Research - UFZ, Department of Computational Hydrosystems, Leipzig, Germany
[e] University of Castilla-La Mancha, Department of Environmental Sciences, Toledo, Spain

HIGHLIGHTS

- We assessed effects of climate-driven warming and flow change on Mediterranean trout.
- We combined climate projections with hydraulic, bioenergetic and eco-genetic models.
- Under warming alone, compensatory dynamics prevented population extinction.
- With warming and flow change, bioenergetic impacts overwhelmed compensatory responses.
- Assuming warming increases food production did not offset impacts of climate change.

GRAPHICAL ABSTRACT
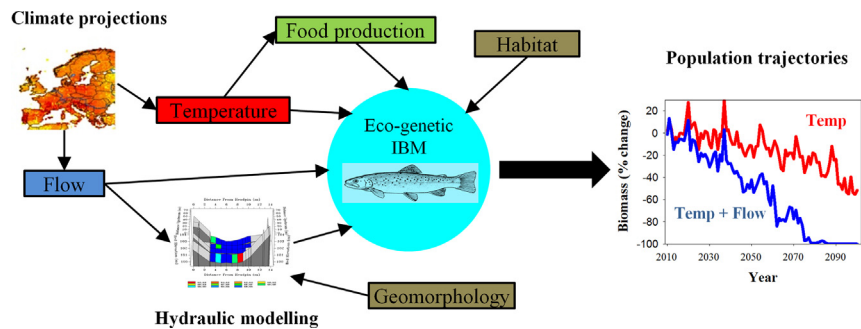
ARTICLE INFO

ABSTRACT

Streamflow is a main driver of fish population dynamics and is projected to decrease in much of the northern hemisphere, especially in the Mediterranean region, due to climate change. However, predictions of future climate effects on cold-water freshwater fish populations have typically focused only on the ecological consequences of increasing temperatures, overlooking the concurrent and interacting effects of climate-driven changes in streamflow regimes. Here, we present simulations that contrasted the consequences of changes in thermal regime alone versus the combined effects of changes in thermal regime and streamflow for resident trout populations in distinct river types with different sensitivities to climatic change (low-altitude main river vs. high-altitude headwaters). We additionally assessed the buffering effect of increased food production that may be linked to warming. We used an eco-genetic individual-based model that integrates the behavioural and physiological effects of extrinsic environmental drivers –temperature and flow– with intrinsic dynamics – density-dependence, phenotypic plasticity and evolutionary responses – across the entire trout life cycle, with Mediterranean brown trout *Salmo trutta* as the model species. Our simulations indicated that: (1) Hydrological change is a critical dimension of climate change for the persistence of trout populations, in that neither river type supported viable populations under strong rates of flow change, even under scenarios of increased food production. (2) Climate-change-related environmental change most affects the largest, oldest trout via increased

---

* Corresponding author at: Complutense University of Madrid, Faculty of Biology, Department of Biodiversity, Ecology and Evolution, José Antonio Novais 12, 28040 Madrid, Spain.
E-mail address: daniel.ayllon@bio.ucm.es (D. Ayllón).

metabolic costs and decreased energy inputs. In both river types, populations persisted under extreme warming alone but became dominated by younger, smaller fish. (3) Density-dependent, plastic and evolutionary changes in phenology and life-history traits provide trout populations with important resilience to warming, but strong concurrent shifts in streamflow could exceed the buffering conferred by such intrinsic dynamics.

1. Introduction

While resident stream fish are currently responding to anthropogenic climate warming at a greater rate than many terrestrial organisms, most species have not shifted their ranges fast enough to track their changing climate (Comte and Grenouillet, 2013). Cold-adapted species face particular challenges in the combination of climate change and more localized anthropogenic environmental modifications (Grenouillet and Comte, 2014). As a result of climate change, many trout species are undergoing changes in distribution and population declines, sometimes to extinction, especially near the southern edge of their range or at low altitudes (Almodóvar et al., 2012; Ayllón et al., 2013; Eby et al., 2014). Projected climatic changes will constrain trout populations to ever smaller and more fragmented headwater habitats. This situation has motivated efforts to identify climate refugia and design effective conservation networks (e.g., Isaak et al., 2015).

Outside of climate refugia, the probability of persistence depends not only on climatic exposure but also on the species' sensitivity and adaptive capacity to climatic changes. The small number of documented extinctions of trout populations to date suggests these populations can exhibit resilience even at low abundances (Kovach et al., 2016). Indeed, adaptive changes in phenology and life-history traits in response to climate change have been extensively documented in salmonids (Crozier and Hutchings, 2014). Of course, local persistence will be possible only if adaptation rates match the rates of environmental change and the population possesses sufficient additive genetic variability to respond adaptively to such changes.

To date, most analyses of climate change effects on resident trout populations have focused only on altered thermal regimes and overlooked the potential impacts of climate-driven shifts in streamflow (Filipe et al., 2013; Kovach et al., 2016), although with rare exceptions (e.g., Wenger et al., 2011; Wade et al., 2017). This is an important omission because summer streamflow has been more consistently related to trout demography and individual growth than temperature (Kovach et al., 2016), and in areas where rainier winters are predicted, statistical species distribution models suggest that increased flood frequency might be a key driver of trout habitat loss (Wenger et al., 2011).

Streamflow is projected to decrease in many areas of the northern hemisphere, but especially in Mediterranean regions (Schewe et al., 2014), where trout will also likely be affected by other drivers of global change such as land use change (Foley et al., 2005). Water availability is indeed the most critical environmental filter for the local persistence of fish populations (Palmer et al., 2009); in particular, flow determines the quality and quantity of available physical habitat and thus the carrying capacity of salmonid populations (Ayllón et al., 2012; Sundt-Hansen et al., 2018). Smaller streams may exhibit greater sensitivity to flow reductions, because wetted area and critical hydraulic features (water depth and velocity) show strong non-linear relationships with flow and the rate of loss is steepest at low flows (Rosenfeld, 2017).

Streamflow also controls the availability of invertebrate drift and thus the magnitude of energy flux to stream-rearing salmonids, consequently influencing their growth, survival and abundance (Harvey et al., 2006; Naman et al., 2016). Field experiments indicate that synergistic interactions between flow-mediated food reduction and elevated temperature increase trout mortality (Bruder et al., 2017). The rate of change in food availability during high- and low-flow events is strongly mediated by channel architecture, specifically cross-sectional profile (e.g. Naman et al., 2017). Therefore, the energetic effects of reduced flow to trout populations will differ along the altitudinal gradient in a river basin as channel morphology changes. As a result, flow-related changes in energy flux can potentially follow a different trajectory than available physical habitat (Rosenfeld, 2017), and thus the overall consequences of changes in streamflow on trout population dynamics are complex and not easy to generalize. While headwaters will be more resistant to warming due to the slower climate velocities of mountain streams (Isaak et al., 2016), it is not evident that they will show a lower sensitivity to climate change if they also undergo hydrological changes. The bioenergetic effects of temperature and streamflow are to some extent confounded, especially during summer low flows when higher temperatures increase energy demand as lower flows reduce food availability. The overall outcome of these interactions for trout survival and growth will be difficult or impossible to predict from empirical data alone (Kovach et al., 2016).

Here, we assess the vulnerability to climate change of resident trout populations living in two river types that differ in their sensitivity to warming and hydrological change. We use a comprehensive mechanistic modelling framework that integrates the behavioural and physiological effects of extrinsic environmental drivers with intrinsic dynamics – density dependence, phenotypic plasticity and evolutionary responses– across the entire trout life cycle. We parameterize the model for two Mediterranean brown trout *Salmo trutta* populations at the warmest edge of the species distribution. We specifically evaluate: (1) how warming and changes in the flow regime (a) affect metabolic, life-history and phenological traits of individual fish through changes in their physical (thermal conditions, habitat availability and hydraulic geometry) and biological (food availability) environment, and (b) how these effects scale up to population dynamics; and (2) the potential of temperature-driven increased food production to buffer the direct (via behaviour and physiology of individuals) and indirect (via habitat and energy fluxes) climate-induced impacts on fish populations.

2. Materials and methods

2.1. Model description

We used inSTREAM-Gen (Ayllón et al., 2016), an eco-genetic version of the individual-based trout model inSTREAM (Railsback et al., 2009). In this model, the demographic and genetic trajectories of trout populations emerge from the growth, survival and reproduction of individual fish, processes driven by complex interactions among temperature and flow conditions, heterogeneous physical habitat, competition for food and habitat, and adaptive behaviour. Plastic responses in growth rates, maturation schedules and phenology can also emerge from natural or anthropogenic biotic or abiotic changes in the environment. InSTREAM-Gen and its documentation can be freely downloaded (https://github.com/DanielAyllon/inSTREAM-Gen-Fishing-version); Appendix A provides a detailed model description that follows the ODD (Overview, Design concepts, Details) protocol (Grimm et al., 2006, 2010). Here, we provide an overview of the model, with focus on the bioenergetics submodel that relates growth and starvation mortality to food availability, temperature, and behaviour.

InSTREAM-Gen simulates the complete trout life cycle using a daily time step, with stream flow and water temperature as environmental drivers. There are four kinds of entities: the stream reach, cells, trout and redds. The model explicitly describes one stream reach of variable length and width, which is divided into cells that represent patches of

relatively uniform habitat. Cells contain information about their physical habitat (water depth and velocity, availability of cover for feeding and avoiding predators), and their production rate of drift and benthic (search) food. On each simulated day, the reach's daily flow and temperature values are updated from input files and the depth and velocity of individual cells are calculated from the flow. Food availability in each cell is subsequently calculated from its physical habitat features and the reach's food parameters. Drift food production rate is modelled as the rate at which prey items flow into the cell from upstream and are regenerated within the cell:

$$
\begin{aligned}
driftHourlyCellTotal \left[\text{g h}^{-1}\right] = {} & 3600 \left[\text{s h}^{-1}\right] \times cellDepth \ [\text{cm}] \\
& \times cellVelocity \ [\text{cm s}^{-1}] \times cellArea \ [\text{cm}^2] \\
& \times habDriftConc \ [\text{g cm}^{-3}]/habDriftRegenDist \ [\text{cm}]
\end{aligned}
$$
(1)

where $habDriftConc$ and $habDriftRegenDist$ are calibrated reach parameters representing the drift food density in the reach and the drift regeneration distance, respectively.

Habitat cells provide benthic (search) food at a rate determined by their area and a calibrated reach parameter that defines benthic food production:

$$
\begin{aligned}
searchHourlyCellTotal \left[\text{g h}^{-1}\right] = {} & habSearchProd \left[\text{g cm}^{-2} \text{ h}^{-1}\right] \\
& \times cellArea \ [\text{cm}^2].
\end{aligned}
$$
(2)

Therefore, when reach-scale drift concentrations and benthic productions rates are constant over time, daily variation in total drift food availability depends on both the reach's wetted area and hydraulics, but benthic food availability only depends on variation in wetted area.

After cells variables are updated, individual trout execute the following actions on each time step:

(1) All trout select a cell for feeding, following a size-based dominance hierarchy that gives larger trout first access to food and preferred habitat. Each trout moves to the available cell, within a radius that increases with body length, that maximizes short-term fitness, which is a function of the cell's mortality risk and growth potential (Railsback et al., 1999). The habitat selection trait is the key adaptive behaviour of trout in the model.

(2) Trout feed and grow according to their food intake and respiration costs experienced in their cell, which are calculated through a bioenergetics model. A fish captures drift food only within a reactive distance that increases with body length but decreases with water velocity, while the amount of food passing within the reactive distance increases with water velocity and drift concentration. Search food intake increases linearly with benthic food production and decreases linearly with water velocity. Respiration is modelled as the energetic costs of metabolism and swimming, including (a) standard respiration that is a function of fish size and water temperature but independent of the fish's activity, and (b) an additional activity respiration that increases with swimming speed, which equals the cell's water velocity. However, cover (e.g., boulders or logs that create local velocity reductions) lower swimming costs for drift-feeding fish, so trout may compete for it:

$$
\begin{aligned}
respTotal \left[\text{j d}^{-1}\right] = {} & respStandard \left[\text{j d}^{-1}\right] \\
& + respActivity \left[\text{j d}^{-1}\right]
\end{aligned}
$$
(3)

$$
\begin{aligned}
respStandard = {} & \left(fishRespParamA \times (fishWeight)^{fishRespParamB}\right) \\
& \times \text{e}^{(fishRespParamC \times temp)}
\end{aligned}
$$
(4)

$$
\begin{aligned}
respActivity = {} & (feedTime/24) \\
& \times \left(\text{e}^{(fishRespParamD \times swimmSpeed)} - 1\right) \\
& \times respStandard
\end{aligned}
$$
(5)

As a result of this formulation, changes in water velocity affect only activity respiration, while changes in temperature affect both standard and activity respiration. Therefore, the daily growth rate experienced by a trout in a cell depends on its body size, the reach's temperature and characteristics of the cell (food and shelter availability, and hydraulic conditions; Fig. B.1 in Appendix B).

(3) Each trout is subject to six natural sources of mortality: starvation, predation by terrestrial animals, predation by piscivorous trout, high temperatures, high velocity, and stranding; the daily probability of surviving each mortality source depends on the state of the fish and the characteristics of its cell. Specifically, the risk of starvation is a function of body condition, while the risk of predation by terrestrial animals (the most common cause of mortality) can be reduced by smaller fish size, hiding cover, and high velocity or depth, and thus is affected by stream flow. Unlike Ayllón et al. (2018a), we did not represent angling mortality.

The next actions take place daily only during specific periods of the year:

(4) Trout become mature when their length reaches their maturity size threshold. During the spawning season, mature females with healthy body condition spawn when environmental conditions (temperature, and flow magnitude and steadiness) allow. Spawning females create a nest (redd) and its eggs are fertilized by the largest available mature male plus a random number of smaller subordinate males. The number of eggs increases exponentially with female length and also varies inversely with egg size. Egg size increases with the genotypic value of the female's trait for length at emergence (see below). Each redd stores the genetic information of the mother and all contributing males.

(5) Redds are subject to egg mortality due to superimposition (placement of a new redd on top of an existing one), and extreme temperatures and flow events (low flows, and scouring at high flows). Surviving eggs develop at a rate that increases non-linearly with temperature.

(6) After redds fully develop, new trout emerge with the heritable traits of length at emergence and the sex-specific maturity size threshold. Each new trout inherits its genetic traits from the mother and one father randomly chosen from the contributing males. The phenotype of an individual is modelled as the sum of an inherited additive genetic effect (genotypic value) and a non-heritable environmental effect; these inheritance rules are based on the infinitesimal model of quantitative genetics (Lynch and Walsh, 1998).

2.2. Study sites

We parameterized the model for resident brown trout populations living in two contrasting river reach types in the same basin in northern Spain. One reach represents a site on the River Eska, the main river of the study basin, which corresponds to the Mediterranean medium-sized mountain river-reach type described in Ayllón et al. (2010), hereafter referred to as "main river". The second reach models a tributary to the River Eska, a medium-sized mountain headwater stream (hereafter referred to as "headwaters").

The sites differ markedly in water temperature and stream flow (Fig. 1). Annual maximum temperatures in the main river (mean 18.1

°C, range 16.8–20.3 °C over 1993–2011) can exceed values at which negative effects on feeding and growth have been observed for brown trout (e.g., 19.5 °C according to Elliott and Elliott, 2010). Annual maximum temperatures in the headwaters (mean 17.0 °C, range 15.7–19.2

°C over 1993–2011) do not reach that values. Flow at the main river site is typically about three times flow at the headwater site (main river: mean annual flow 4.28 m³ s⁻¹, mean summer flow 0.71 m³ s⁻¹, minimum flow 0.39 m³ s⁻¹; headwaters: mean annual flow
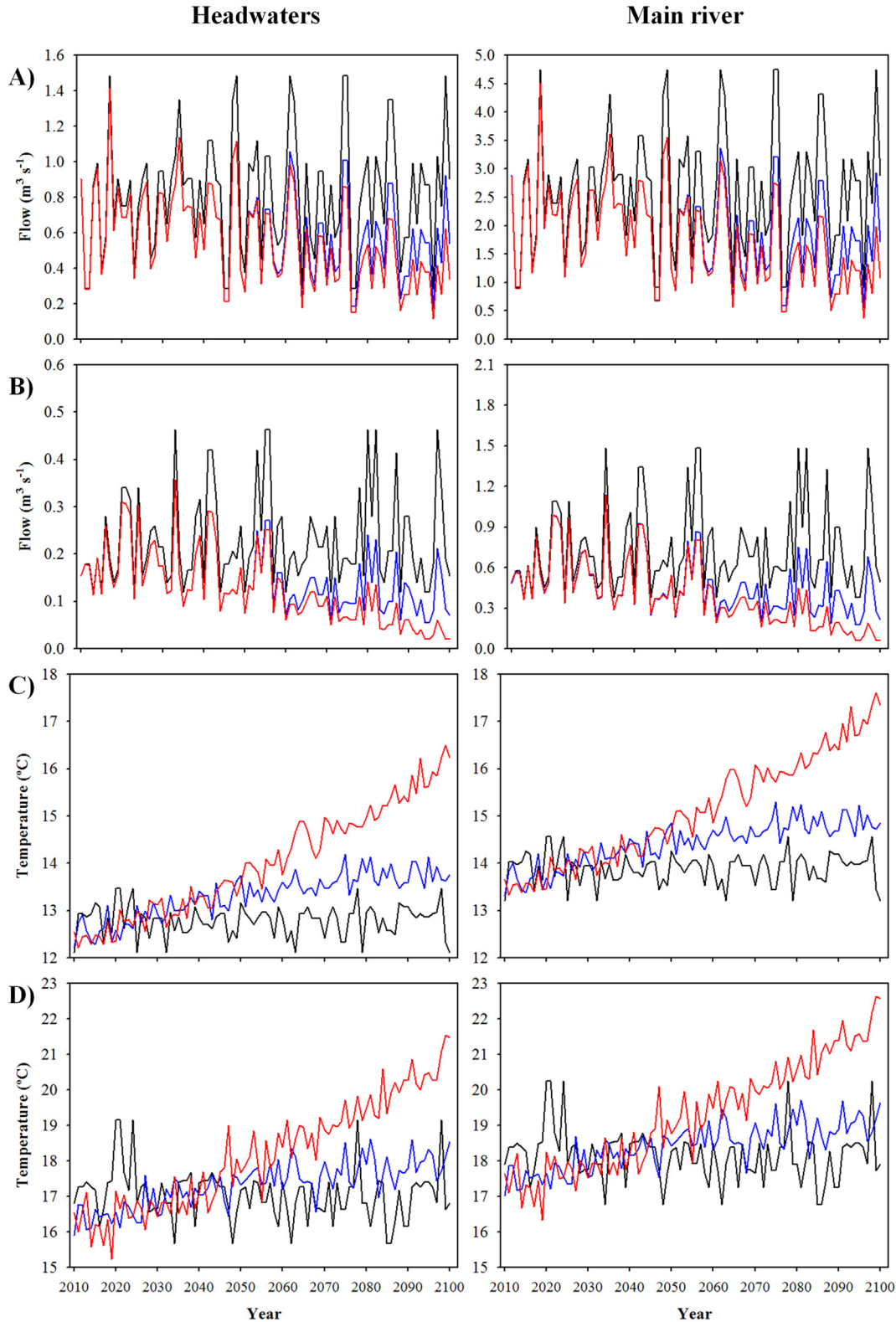

Fig. 1. Time series of mean daily flow (row A) and seven-day minimum daily flow (row B) during the trout growing season (March to October) under the no-flow-change (baseline, RCPs 4.5 and 8.5; black line), RCP4.5 + Flow change (blue line) and RCP8.5 + Flow change (red line) simulation scenarios. Time series of mean daily temperature (row C) and seven-day maximum daily temperature (row D) during the trout growing season under the baseline (black line), RCP4.5 (and RCP4.5 + Flow change; blue line) and RCP8.5 (and RCP8.5 + Flow change; red line) scenarios. (For interpretation of the references to colour in this figure legend, the reader is referred to the web version of this article.)

1.38 m^3 s^{-1}, mean summer flow 0.23 m^3 s^{-1}, minimum flow 0.13 m^3 s^{-1}).

Basin- and reach-scale morphological features and hydraulic geometry also differ between the reach types (Table 1). The main river reach has a higher ratio of drainage area to river length, which produces a U-shaped channel, in contrast to the headwaters reach's V shape. The width-to-depth ratio, a good descriptor of channel shape, is almost three times higher in the main river; the headwaters channel is narrower and more constrained by bedrock (Table 1; Fig. B.2). The main river has a higher proportion of fast waters to pool habitat than the headwaters and higher mean water velocity but lower water depth (Table 1).

Topographic, hydraulic, and structural data required to describe study sites in inSTREAM-Gen were collected following standard procedures: total depth, current velocity, substrate composition and cover were measured every 1 m along transects placed perpendicular to the flow. The proportion of different substrate (silt, sand, gravel, cobble, boulder and bedrock) and cover (velocity shelters, aquatic and overhanging vegetation, woody debris and undercut bank) types were visually estimated in 1-m^2 quadrats. We used hydraulic models of PHABSIM v.1.5.1 (Milhous and Waddle, 2012) to obtain the functions relating cell-specific depths and velocities to total streamflow. Site-specific demographic and life-history data required to characterize the model populations were obtained from previous field studies (e.g., Ayllón et al., 2012, 2013; Parra et al., 2014). Characteristics of the initial population (mean and standard deviation of length-at-age and age-specific abundance) were based on field data collected by the Government of Navarre in 1993. Model parameterization is extensively described in Appendix C.

2.3. Simulation scenarios

We simulated trout populations between 1993 and 2100 under five different environmental scenarios. We generated time series for water temperature and flow for that period in a two-step process. We used recorded data from the closest stream gauging (Isaba, Navarra Government) and meteorological (Urzainqui, AEMET) stations to generate flow and water temperature time series for the 1993–2011 period. Time series over 2012–2100 were projected for each scenario following the methodology fully described in Ayllón et al. (2016) and summarized below.

2.3.1. Baseline scenario

We modelled a baseline scenario that continues the historical temperature and flow regimes without climate change. We first analysed the entire historic time series (1992–2011) from the Isaba gauging station using IHA v7.1 software (The Nature Conservancy) to differentiate years into five flow-event categories and determine their probability of occurrence: extreme low flows (probability of occurrence within the

analysed time series = 0.158), low flows (0.368), small floods (0.368), large floods (0.053), and extreme low flows in summer concurrent with large floods in winter (0.053). The last category reflects the most extreme intra-annual variability in flow conditions. The flow regime for each year of the 2012–2100 time period was randomly set to one of those initial years (1992–2011), using probabilities weighted to reproduce the historic frequency of flow-events categories. We estimated water temperature time series from air temperature time series using a linear regression model specifically developed for the Aragón River basin (see Ayllón et al., 2016): $T_{water} = 3.331 + 0.633 \cdot T_{7d\text{-}air}$, where T_{water} is daily water temperature and $T_{7d\text{-}air}$ is the mean air temperature during the previous seven days. Air temperature time series at the study reaches were derived from the Urzainqui meteorological station's time series by means of the regional air temperature model ($T_{7d\text{-}air}$ [°C] = 323.25–6.914·Latitude [decimal degree] − 0.0044·Altitude [m]) described in Ayllón et al. (2013). The air temperature time series for 2012–2100 were projected by using historical data from the same year as for the flow regime to avoid unnatural decoupling of environmental variables.

2.3.2. Scenarios of environmental change

2.3.2.1. Climate warming scenarios.
The first set of scenarios represent temperature increases due to climate warming but not changes in flow, so we used the same flow time series developed for the baseline scenario. We used two future climate projections corresponding to the Representative Concentration Pathways RCP4.5 and RCP8.5 (Taylor et al., 2012) to generate the temperature time series. Under the RCP4.5 projection, greenhouse gas emissions peak in 2040 and then decline, so total radiative forcing stabilizes shortly after 2100 without overshooting the long-run radiative forcing target level, resulting in moderate warming. The RCP8.5 is characterized by increasing greenhouse gas emissions over time, leading to high greenhouse gas concentration levels and thus to very strong warming. We used the inter-model median of regional daily air temperature projections for the Urzainqui meteorological station developed by AEMET through statistical downscaling techniques based on data from six global climate models associated with the 5th Coupled Model Intercomparison Project: (1) BCC-CSM1-1 (Beijing Climate Center, China), (2) CanESM2 (Canadian Centre for Climate Modelling and Analysis, Canada), (3) GFDL-CM3 (Geophysical Fluid Dynamics Laboratory, USA), (4) MIROC-ESM-CHEM (Japan Agency for Marine-Earth Science and Technology, Japan), (5) MPI-ESM-LR (Max-Plank Institute, Germany), and (6) MRI-CGCM3 (Meteorological Research Institute, Japan).

Projected air temperatures were translated into water temperatures using the same model as for the baseline scenario. The RCP8.5 scenario projects water temperatures well above 20 °C in both reaches, but such temperatures are projected to be reached much earlier in the main river (Fig. 1C, D).

2.3.2.2. Climate warming & hydrological change scenarios.
These scenarios represent increasing temperature and changes in flow regime due to both climate and land-use change. We used the same water temperature times series described above, developed from RCPs 4.5 and 8.5. Scenarios of hydrological change relied on stream flow projections performed by López-Moreno et al. (2014) for the River Aragón basin (River Eska is tributary to River Aragón) for 2021–2050 under the A1B scenario of moderate greenhouse gas emissions. Temperature predictions under the A1B emission scenario lie between those of the representative concentration pathways 6.0 and 8.5. These flow projections are based on projected temperature and precipitation patterns and the expected evolution of land cover according to observed recent trends of abandonment of agricultural fields and subsequent afforestation, natural re-vegetation and decrease in livestock pressure (see López-Moreno et al., 2014 and references therein). Simulations assume that pasture and shrub areas in the basin will evolve into evergreen conifer

Table 1
Morphological basin-scale descriptors and reach-scale morphological variables measured at the median summer discharge, and water depth and velocity (mean ± standard deviation over wetted cells at the median summer discharge).

Variable	Headwaters	Main river
Watershed descriptors		
Altitude (m a.s.l.)	870	655
Watershed size (km^2)	79	293
Distance from the origin (km)	13	29
Stream order	2	3
Basin shape (km^2 km^{-1})	6.0	10.1
Slope (%)	5.2	0.9
Reach descriptors		
Channel width (m)	6.8	22.5
Width / depth ratio	27.3	83.6
Depth (cm)	22 ± 18.7	18 ± 7.4
Velocity (cm s^{-1})	28.4 ± 25.5	31.4 ± 26.7

forests, and that tree line will shift upward from 1600 to 1800 to 2000 m altitude. López-Moreno and collaborators predicted a continuous decrease in runoff (due to increased plant evapotranspiration and slight decreases in precipitation) from late winter to the end of autumn, with reductions in streamflows exceeding 30–40% relative to the historical baseline, especially in summer.

We designed different scenarios of hydrological change for each of the temperature scenarios. First, we modified daily streamflow from the baseline scenario for 2012–2050 to reflect seasonal changes projected by López-Moreno et al. (2014). Daily flows within each month decreased linearly at a rate calculated to match reductions through 2050 projected by López-Moreno and collaborators. On the basis of projected temperature and precipitation patterns, we assumed that stream flows would continue decreasing over 2051–2100 but at different rates for the two simulated RCP scenarios. We assumed that flows would continue to decrease at the same rate under the RCP8.5 scenario, but for the RCP4.5 scenario we arbitrarily set the flow decrease rate for 2051–2100 to half the rate assumed for 2012–2050. Therefore, we designed a "RCP4.5 + Flow change" scenario of moderate warming and flow reduction, and a "RCP8.5 + Flow change" scenario of very strong warming and flow reduction (Fig. 1A, B).

2.3.3. Scenarios of environmental and food production change

The third set of scenarios include the environmental change described in Section 2.3.2 concurrent with a change in food production over time as a result of the projected warming. In these scenarios, the parameters defining drift and benthic food production at the reach scale (*habDriftConc* and *habSearchProd*, respectively) change every simulated year during 2012–2100 as a function of temperature instead of remaining constant. We used the formula of Morin (1997):

$$\text{Log } P = 2.10 + 0.20 \times \text{ log M} + 0.037 \times \text{T} \tag{6}$$

where P is the expected invertebrate annual production (mgDM m^{-2} y^{-1}), M is individual body mass (mg Dry Mass) and T is mean annual temperature (°C). Morin's formula resulted from the combination of a regression model predicting density from body mass (Morin, 1997) with the model of Morin and Bourassa (1992) predicting production from body mass, biomass and temperature, which were derived from a meta-analysis of 35 and 60 published empirical studies, respectively. These empirical studies encompassed data from a large number of rivers and taxonomic groups. We assumed no changes over time in individual mass and calculated the relative change in food production as a function of the change in temperature under scenarios RCP4.5 and 8.5 relative to a reference temperature (mean annual temperature during the period 1993–2011: 9.8 °C in the headwaters and 10.9 °C in the main river). Therefore, production of food of either type (*habDriftConc* or *habSearchProd*) was calculated each year for 2012–2100 as:

$$F_i = F_0 \times 10^{(0.037 \times (T_i - T_0))} \tag{7}$$

where F_i and T_i are food production and temperature at year i, while F_0 and T_0 are reference values for 1993–2011.

2.4. Model outputs

2.4.1. Physical habitat and food availability

We first assessed the predicted effects of simulated flow changes on the reach physical habitat and the availability of food for trout during the season in which growth is most rapid (March to October; hereafter referred to as the "growing season"). To this end, we recorded each simulated day the reach's wetted area, mean water depth and velocity (weighted by the availability of velocity shelters, so that it represents the swimming speed of fish feeding in the drift) of wetted cells, and the drift, benthic and total food available in the reach. Values were averaged over the growing season.

2.4.2. Fish bioenergetics

We then analysed the predicted effects of simulated temperature and flow changes on fish energy expenditure. For each simulated day, we calculated the standard, activity and total respiration costs for a trout of a size equal to the size maturity threshold swimming at a speed equal to the reach's mean water velocity (see previous Section 2.4.1), and averaged these daily values over the growing season.

2.4.3. Fish life-history and phenology traits, and population demography

Finally, we analysed the predicted consequences of temperature and flow-driven changes in instream physical habitat and fish energetics on individual growth rates and body size traits, and how they scale up to alter the demography and eco-evolutionary trajectory of model populations. For this analysis, we recorded the density, biomass, and mean individual length and weight (W) of four age-classes (0, 1, 2, and 3-and-older trout) every simulated year at September 1st. Growth rate (G_L) was calculated as a daily mass-specific rate $G_L = (\ln W_1 - \ln W_2) (t_2 - t_1)^{-1}$, where W_1 and W_2 are mean W at age at times t_1 and t_2. We calculated this growth rate for age-0 trout during the first growing season (between emergence time and September 1st), during the first annual interval (age-0 –at September 1st– to age-1 years, which mostly reflects trout growth during the growing season as age-1 individuals) and during the second annual interval (age-1 to age-2 years, which mostly reflects trout growth during the growing season as age-2 individuals). The size structure of the population was measured as the adult (trout older than age-1) to juvenile (age-0 and 1 trout) biomass ratio. We also calculated the production rate of the population from emergence to the third year of life using the instantaneous growth method (Ricker, 1975). Production represents the flow of energy across trophic levels to create new tissue over time, so it is quite responsive to environmental change. We additionally recorded at the end of each spawning season the population fecundity (total number of eggs produced). To track the simulated evolution of the populations, we recorded the mean genotypic value of length at emergence of all spawners. We also recorded the mean date of spawning and emergence, measured as the Julian date.

2.5. Data analyses

We evaluated the trajectory of model outputs using the rank-based non-parametric Mann-Kendall test (Mann, 1945; Kendall, 1975), which can detect significant trends over time that need not be linear. This test is robust to outliers, does not assume any distribution of data, and has low sensitivity to abrupt breaks in the series, but it is quite sensitive to serial correlation. The analysis was thus performed as modified by Yue et al. (2002) to account for temporal autocorrelation with the *zyp* v0.10-1 R package (Bronaugh and Werner, 2015). We estimated the Kendall's tau statistic and its probability, and the Sen's slope (the median linear slope joining all pairs of observations) expressed by quantity per unit time.

3. Results

3.1. Physical habitat and food availability

Mean water temperature during the growing season is projected to increase in both river types, by 0.12 and 0.35 °C per decade in the climate warming scenarios RCP4.5 and RCP8.5, respectively. In the simulations with no temperature-driven changes in food production, the average total energy availability (i.e., total energy content of invertebrates both in the drift and in the benthos) during the growing season at the end of simulation time (2086–2100) was 1.4 times higher in the main river than in the headwaters under both warming scenarios.

Both reach wetted area and mean water velocity significantly decreased over time under both warming plus flow-change simulation scenarios (Table 2, Fig. 2). Consistent with the differences in channel morphology between reach types, the rate of decrease in wetted area

was higher in the main river while the rate of change in water velocity was higher in the headwaters.

Benthic food availability decreased significantly over time under both warming plus flow-change simulation scenarios due to the reduction in wetted area, and thus the effect was stronger in the main river (Table 2, Fig. 2). Drift food availability decreased at a faster rate than benthic food availability under both warming plus flow-change scenarios, since it depends both on wetted area and water velocity. Stronger reduction in wetted area in the main river compensated for stronger reduction in water velocity in the headwaters, resulting in similar decreases in drift food in the two reach types (Table 2, Fig. 2). Overall, food availability decreased at a higher rate in the main river (Table 2, Fig. 2). At the end of the simulation period (mean for 2086–2100) under the most extreme scenario (RCP8.5 + Flow change), total food availability decreased by 49% in the main river and by 46% in the headwaters. The average total energy availability during the growing season was only 1.3 times higher in the main river than in the headwaters under the combined scenarios with hydrological change.

When we simulated changes in food production as a function of temperature, food availability increased under temperature-change-only scenarios (of course) and it still decreased under hydrologic change but at a lower rate compared to scenarios in which food production remained constant (Table 3). In fact, temperature-driven food production resulted in increased benthic food availability under the RCP8.5 + FC scenario in both river types, but not under the RCP4.5 + FC scenario.

3.2. Fish energetics

The standard respiration costs for a trout of a given size increased significantly over time relative to the baseline, at a rate of 1.3 and 3.3%

per decade under the RCP4.5 and 8.5 climate warming scenarios, respectively (Table 2, Fig. 3). Due to the reduction in water velocities under the combined warming and flow-change simulation scenarios, the respiration costs associated with swimming increased over time at a lower rate than under warming alone in the main river, and actually decreased over time in the headwaters (Table 2, Fig. 3). Therefore, the increase in total respiration costs under the scenarios simulating both climate warming and hydrological change was markedly lower in the headwaters than in the main river (Table 2, Fig. 3). As a result of these patterns of change over time, under combined warming and flow reductions over the last 15 years of the simulated period, a female at the threshold size for maturity requires around 2.6 times more energy for maintenance and feeding in the main river than in the headwaters, while the potential energy intake is only around 1.3 higher in the main river (see Section 3.1).

3.3. Fish phenology and life-history traits

There were density-dependent, plastic and evolutionary responses in fish individual traits that helped reduce the effects of changes in temperature and stream flow:

1) We detected a strong genetic response towards smaller size at emergence, especially in the combined scenarios of warming and flow change, particularly in the main river (Table 2). Larger size at emergence was linked to reduced growth rates of age-0 trout during their first growing season (Table D.1 in Appendix D). Moreover, because of the tradeoff between number of eggs produced and egg size (see Model description), larger eggs (and thus size at emergence) reduce fecundity.

2) Changes in the environment affected trout phenology (Table 2). Fish emerged earlier due to faster development of eggs resulting from

Table 2

Trends of model outputs over the 1994–2100 time period for the climate warming (RCPs 4.5 and 8.5) and climate warming plus flow change (RCP 4.5 and 8.5 + Flow change) simulation scenarios in two river types (headwaters vs. main river). Trends were analysed using the Mann-Kendall test and *p*-values were corrected for serial correlation. Trends are represented as the Sen's slope in %/decade. All trends were highly significant ($P < 0.001$) except when indicated otherwise (ns non-significant, * $P < 0.05$, ** $P < 0.01$).

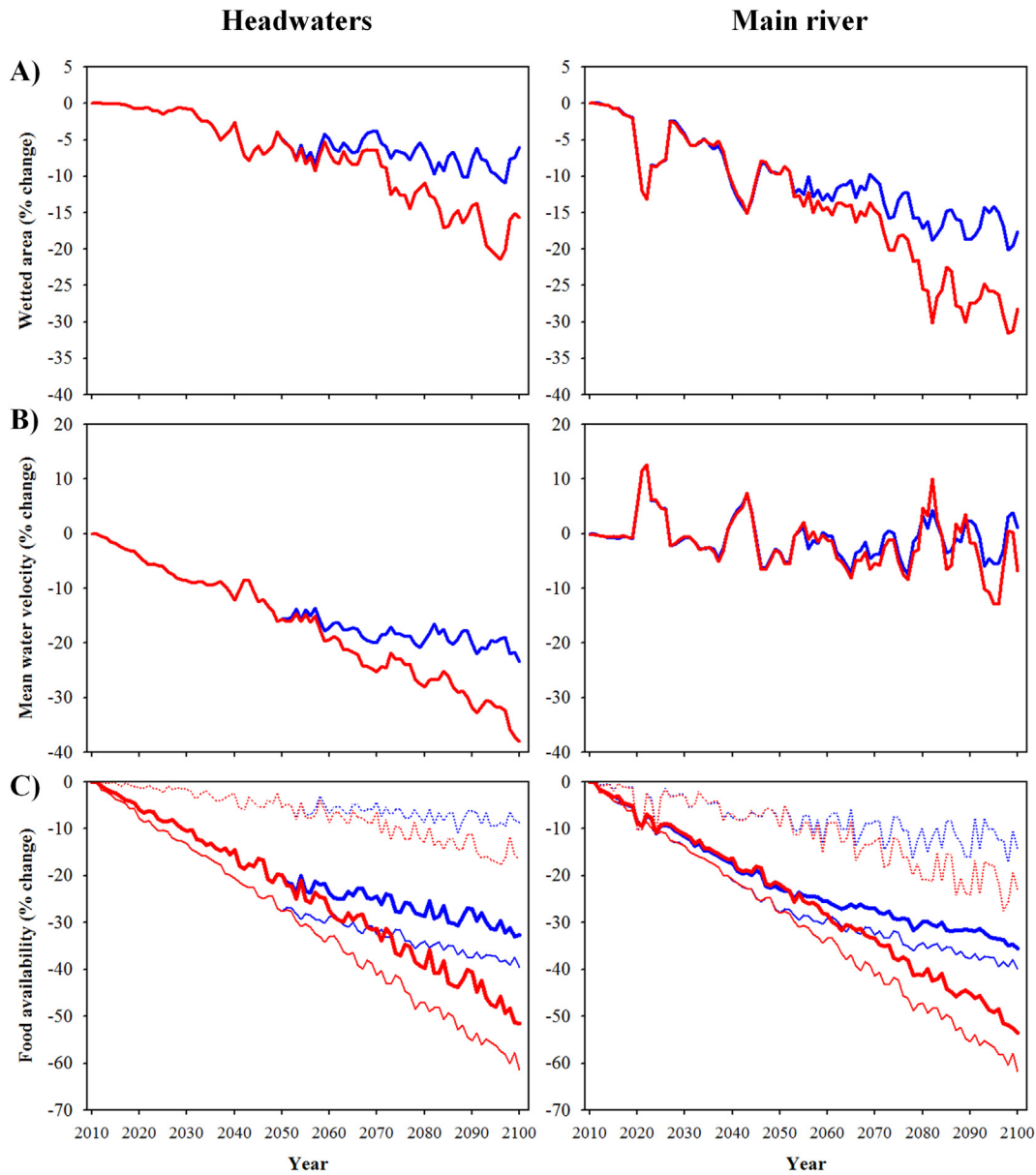|	Headwaters				Main river			
	RCP4.5	RCP8.5	RCP4.5FC	RCP8.5 FC	RCP4.5	RCP8.5	RCP4.5FC	RCP8. 5FC
Physical habitat								
Wetted area	0 ns	0 ns	−0.89	−1.77	0 ns	0 ns	−1.60	−2.74
Water velocity	0 ns	0 ns	−2.45	−3.56	0 ns	0 ns	−0.44	−0.80
Food availability								
Drift food	0 ns	0 ns	−4.31	−6.52	0 ns	0 ns	−4.33	−6.50
Benthic food	0 ns	0 ns	−0.91	−1.55	0 ns	0 ns	−1.37	−2.19
Total food	0 ns	0 ns	−3.48	−5.22	0 ns	0 ns	−3.74	−5.73
Metabolic traits								
Standard respiration	1.32	3.33	1.32	3.33	1.32	3.33	1.32	3.33
Activity respiration	1.32	3.33	−1.94	−2.01	1.32	3.33	0.63	1.76
Total respiration	1.32	3.33	0.30 *	1.60	1.32	3.33	1.10	2.77
Phenological traits								
Spawning date	0.07 ns	0.16	0.23	0.94	0.04 ns	0.13	−0.01 ns	0.36 **
Emergence date	−1.66	−3.42	−0.87 *	−0.04 ns	−1.69	−3.06	−1.83	−1.42 ns
Body size traits								
Gen Emergence L	0.09	−0.09	−0.35	−0.24	−0.34	−0.42	−0.52	−0.68
Growth rate age-0	−0.94	−1.74	−0.04 ns	0.22 ns	−0.40 **	−0.47 **	−0.95	0.58 ns
Growth rate age-1	−0.57	−0.83	−0.41 **	1.68	−0.03 ns	−0.30 **	−0.47 *	−1.13
Growth rate age-2	0.27 **	0.43	0.68	−2.65 *	−0.84 *	−1.64	0.09 ns	−1.71 *
Weight age-0	0.62 *	1.04	0.58 ns	5.78	0.83	2.71	−0.77 ns	3.57 *
Weight age-1	−0.10 ns	−0.06 ns	0.06 ns	6.46	0.76	1.95	−1.88	−0.14 ns
Weight age-2	0.23 ns	0.31 ns	0.86 *	3.35	0.01 ns	0.23 ns	−2.02	−1.60
Weight age > 2	−0.36 *	−1.85	−2.99	−3.75	−0.30 ns	−0.76	−4.64	−5.67
Demography								
Production	−2.07	−5.56	−7.75	−12.00	−3.98	−8.09	−9.91	−12.27
Total biomass	−1.11	−3.21	−4.84	−10.05	−1.70	−4.27	−7.61	−11.82
Ratio adults/juveniles	−0.75	−2.11	−4.18	−6.46	−2.72	−5.17	−6.58	−10.51
Total fecundity	−1.01	−3.56	−6.03	−11.77	−2.82	−7.11	−9.25	−11.59

Headwaters

Main river

Fig. 2. Change over time in the physical habitat and food availability variables under scenarios of flow change relative to the baseline scenario in two river types (headwaters vs. main river). The figure shows wetted area (row A) and mean water velocity (row B) changes under RCP4.5 + Flow change (blue line) and RCP8.5 + Flow change (red line) scenarios. Row C shows the availability of drift (thin continuous line), benthic (dotted line) and total food (thick continuous line) changes under RCP4.5 + Flow change (blue colour) and RCP8.5 + Flow change (red colour) scenarios. Changes in the variables are expressed as the percentage change: [(value flow change scenario − value baseline) / value baseline] × 100. Time series were smoothed using the three-year moving average for representation purposes. (For interpretation of the references to colour in this figure legend, the reader is referred to the web version of this article.)

increased temperatures, which lengthened their first growing season. However, increased temperatures and decreased flows in late autumn and early winter delayed spawning under the combined scenarios, more markedly in the headwaters (due to lower flow magnitude). Overall this yielded similar dates of emergence under the baseline and RCP8.5 + Flow change scenarios.

3) Due to increased metabolic costs and reduced energy availability, daily growth rates of age-0 trout during their first growing season decreased over time (Table 2). However, decreased competition for safe and productive feeding sites (see Section 3.4) resulted in density-dependent growth responses that partially (or totally) compensated for increased metabolic costs (Table D.1). Growth rates of age-1 trout showed similar compensatory dynamics (Table D.1). Patterns of age-2 trout growth rates differed between

river types because of the large differences in metabolic demands, which made density-dependent compensation impossible in the main river; therefore, while growth in the headwaters increased over time under all but the most extreme scenario (RCP8.5 + Flow change), growth in the main river decreased over time in all environmental change scenarios (Table 2). Because daily growth rates decreased in general, production rates were more affected by climate change than total population biomass in both river types (Table 2).

4) These differences in growth trajectories led to different size-at-age patterns among age classes and river reach types (Table 2). The most consistent patterns were that age-3 and older trout became smaller over time while age-0 trout became larger because earlier emergence offset reduced daily growth rates (Table D.2).

Table 3

Trends of model outputs over the 1994–2100 time period for the climate warming (RCPs 4.5 and 8.5) and climate warming plus flow change (RCP 4.5 and 8.5 + Flow change) simulation scenarios concurrent with simulated changes in food production in two river types (headwaters vs. main river). Methods and format are the same as for Table 2.

	Headwaters				Main river			
	RCP4.5	RCP8.5	RCP4.5FC	RCP8.5 FC	RCP4.5	RCP8.5	RCP4.5FC	RCP8. 5FC
Food availability								
Drift food	1.16	3.41	−3.63	−4.84	1.16	3.41	−3.66	−4.86
Benthic food	1.16	3.41	0.08 *	1.23	1.16	3.41	−0.40	0.43
Total food	1.16	3.41	−2.73	−3.19	1.16	3.41	−3.12	−4.03
Body size traits								
Gen Emergence L	0.26	0.40	−0.10 *	0.06 *	−0.07 *	0.02 ns	−0.55	−0.51
Growth rate age-0	−0.58	−1.22	0.05 ns	0.51 **	−0.15 ns	0.16 ns	0.49 ns	1.50
Growth rate age-1	−0.26 ns	0.29 ns	0.48 **	1.77	0.14 ns	0.16 ns	−0.24 ns	−0.63 **
Growth rate age-2	0.46 *	1.20 *	0.73 **	0.11 ns	−0.77 *	−1.61	−1.65	−5.04
Weight age-0	2.68	7.18	2.90	8.02	2.69	7.80	2.40	11.00
Weight age-1	2.29	8.90	3.56	14.33	3.07	9.17	1.50	7.21
Weight age-2	3.09	10.81	4.36	13.26	1.86	6.08	−0.19 ns	1.20
Weight age > 2	2.99	10.50	0.34 ns	4.09	1.46	5.78	−2.84	−3.09
Demography								
Production	−0.04 ns	−0.89 ns	−5.91	−11.16	−2.74	−5.29	−9.67	−11.98
Total biomass	0.39 ns	0.81 ns	−3.12	−6.21	−0.52 ns	−0.71 ns	−6.52	−11.19
Ratio adults/juveniles	−0.58 *	−1.31	−3.88	−7.04	−3.05	−5.68	−7.30	−10.45
Total fecundity	2.60	4.89	−5.32	−12.01	0.65 ns	1.55 ns	−9.05	−11.75

3.4. Population-level responses

Age-specific density and biomass decreased significantly over time under the various climate change scenarios (Table E.1 in Appendix E). Both decreased more severely with age and the addition of hydrologic change to temperature change. Decreases in the main river exceeded those in the headwaters except for age-0 trout, because stronger mortality rates in older age classes relaxed inter-cohort competition for resources. Therefore, the production rate, biomass, ratio of adult to juvenile biomass, and fecundity of the population decreased significantly over time in both reach types under all simulated scenarios and declining rates were stronger in the main river (Table 2). Populations in both reaches went extinct under the most extreme scenario (RCP8.5 + Flow change), but earlier in the main river (in simulated year 2087 vs. 2096; Fig. 4). However, reproduction fell almost to zero much earlier, beginning in the 2060s in the main river and the 2070s in the headwaters (Fig. B.3 in Appendix B). Besides, declining rates in fecundity, biomass and production indicated proximate extinction in the main river population under the other combined scenario (RCP4.5 + Flow change) while the population in the headwaters appeared more stable (Table 2; Fig. 4).

3.5. Individual and population responses to changes in food production

Temperature-driven increases in food availability led to higher average growth rates of trout during their first and second growing seasons in both river types under all scenarios. Daily growth rates during the third growing season also increased under all scenarios in the headwaters. In consequence, the size at age of all age classes increased over time in almost all simulation scenarios and the simulated fish attained bigger sizes than under the scenarios with no changes in food production. However, the increase in food availability was not enough to offset the increased metabolic demands of such large fish in the main river with its higher temperatures, and thus the daily growth rates during the third growing season decreased at a faster rate than under the scenarios with no changes in food production (Tables 2 and 3).
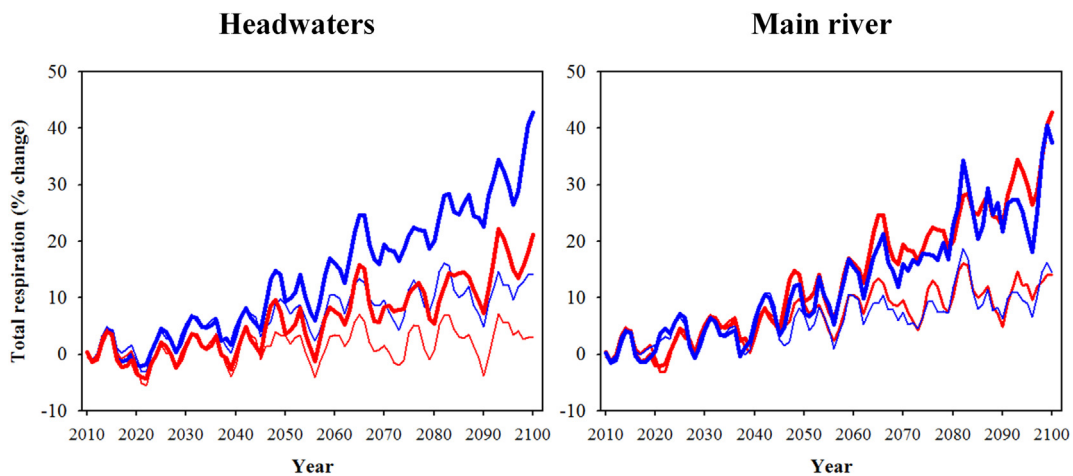

Fig. 3. Change over time in total respiration costs under the RCP4.5 (blue thin line), RCP8.5 (blue thick line), RCP4.5 + Flow change (red thin line) and RCP8.5 + Flow change (red thick line) scenarios. Changes in respiration costs are expressed as the percentage change: [(value environmental change scenario − value baseline) / value baseline] × 100. Time series were smoothed using the three-year moving average for representation purposes. (For interpretation of the references to colour in this figure legend, the reader is referred to the web version of this article.)
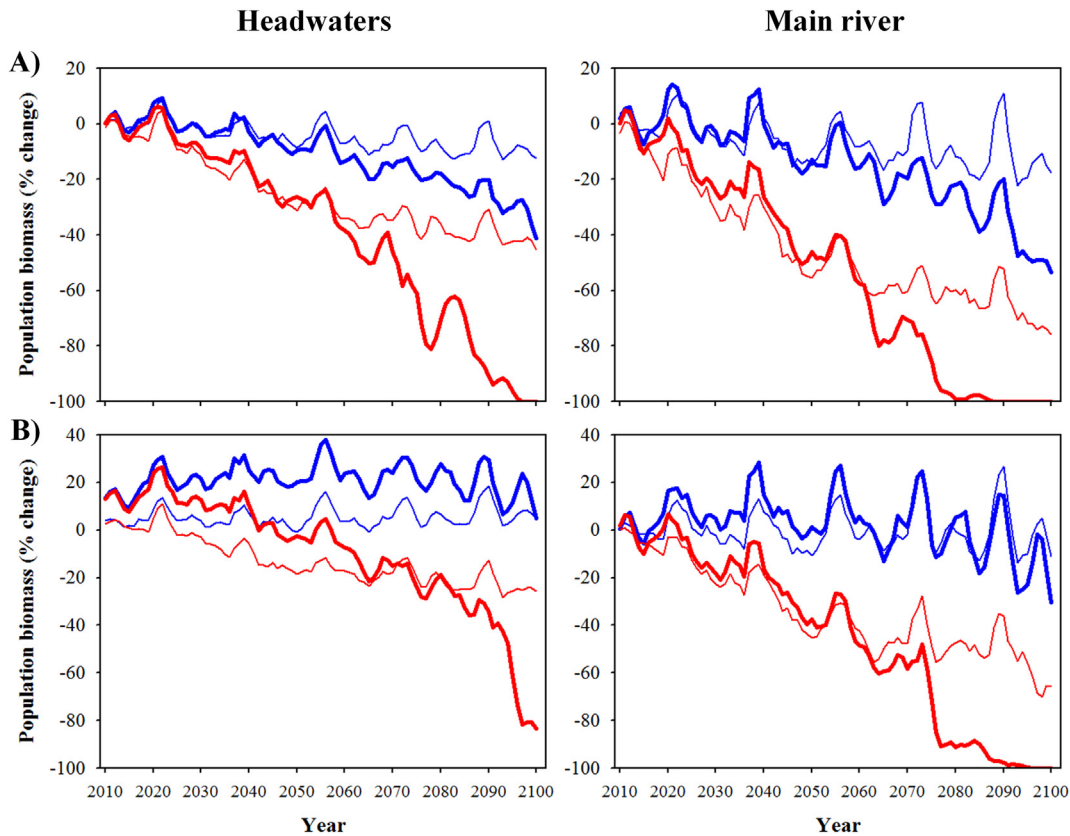
Fig. 4. Change over time in population biomass under scenarios of environmental change without (A) and with simulated increase in food production (B) relative to the baseline scenario in two river types (headwaters vs. main river). Biomass change was simulated under the RCP4.5 (blue thin line), RCP8.5 (blue thick line), RCP4.5 + Flow change (red thin line) and RCP8.5 + Flow change (red thick line) scenarios. Changes in biomass are expressed as the percentage change: [(value environmental change scenario − value baseline) / value baseline] × 100. Time series were smoothed using the three-year moving average for representation purposes. (For interpretation of the references to colour in this figure legend, the reader is referred to the web version of this article.)

Increasing food production had strong positive effects on simulated cohort production, population biomass and fecundity in both river types under the two temperature-change-only scenarios (Tables 2 and 3). However, the buffering effect of increasing food production was limited under combined scenarios of warming and flow change, especially in the main river (Tables 2 and 3). The assumption of increased food production with temperature delayed but did not prevent extinction under the worst case scenario (RCP8.5 + FC) (Fig. 4).

4. Discussion

Comprehensive assessment of trout vulnerability to future conditions requires quantification of future climatic exposure, and a clear understanding of both the aspects of climate change that influence fish vulnerability across life-stages and the capacity of the fish to adjust to the changing climate (Wade et al., 2017). Assessments of vulnerability also must include the ability to address the effects of interacting drivers of population dynamics. Here, our simulations suggest that: (1) Hydrological change is a critical dimension of climate change for the persistence of trout populations, in that the combination of strong thermal and hydrologic changes prevented population persistence, even in simulated headwaters and even under scenarios in which we assumed that higher temperatures elevate food production. (2) Largest, oldest trout experience the strongest impacts of increased metabolic costs and decreased energy inputs; extreme warming led in both river types to smaller populations dominated by young individuals but not to extinction. This suggests that flow-induced energy limitation would be the proximate factor leading to extinction under warming conditions. (3) Density-dependent, plastic and evolutionary changes in phenology and life-history traits provide trout populations with important

resilience to warming –as indicated by the persistence of our simulated populations subjected to warming alone– but strong shifts in streamflow regimes exceed the buffering conferred by such intrinsic dynamics.

Our primary simulation result is that neither population could compensate for the combined effects of extreme warming and flow change; even the moderate scenario led the main river population to extinction. This result withstood the facts that simulated fish could exhibit adaptive behaviour and compensate for environmental change via density dependence, phenotypic plasticity and evolution, although other adaptive capacities (e.g., through shifts in thermal tolerance; Eliason et al., 2011) were not explored in this study. Simulated fish behaviourally adapted to more energetically challenging conditions by selecting more profitable foraging habitat but at the cost of higher predation risk, so overall mortality was not reduced. Both populations exhibited responses that slowed down the rate of decline in abundance and production (see Appendix D), including: (1) high mortality rates elicited strong density-dependent compensatory responses that helped reduce negative effects of environmental changes on growth rates in age-0 and age-1 trout; (2) the interplay of the needs to survive both starvation and terrestrial predation caused selection for smaller size at emergence, because in our model, as in real populations, larger trout have higher metabolic requirements (e.g., Elliott, 1976) and are more susceptible to predation (e.g., Harvey and Stewart, 1991; Hodgens et al., 2004), and because smaller size at emergence comes with higher fecundity (Jonsson and Jonsson, 2011); (3) egg development rates and hence emergence timing responded to temperature, which resulted in stable or increased body size of surviving age-0 trout during their first growing season. (This pattern in body size persisted over the first three years of life, despite increasing metabolic demands.) While adaptive behaviour and intrinsic

dynamics did not prevent extinction under the combination of altered thermal and hydrologic regimes, they did prevent extinction under all scenarios of warming alone.

The inability of response mechanisms to overcome changes in both temperature and streamflow was exacerbated by the fact that not all plastic responses were adaptive. As a consequence of warming and flow decreases in late autumn, fish delayed spawning, which delayed emergence, which reduced the length of the first growing season for new recruits, thus affecting their size at the end of the season. Avoiding one problem worsened another: spawning later to reduce temperature-related mortality of eggs resulted in later emergence and smaller size. While density-dependent effects compensated somewhat for such shifts in phenology, delayed spawning remains a maladaptive response to the changing environment. Others researchers have observed negative consequences of climate-related changes in salmonids phenology. For example, earlier seaward migration (Kennedy and Crozier, 2010) or emergence (Fullerton et al., 2017) can reduce marine and freshwater survival.

Our simulations indicated that responses of growth and survival to temperature and flow changes were age-dependent, consistent with previous predictions (Letcher et al., 2015). Across all our climate change scenarios, the largest, oldest trout experienced the strongest impacts on growth and survival from increased metabolic costs and decreased energy inputs. Both warming alone and concurrent warming and hydrological change produced a shift in age structure, leading to smaller populations dominated by young individuals and thus with a lower mean body size. This is consistent with predictions from temperature-size relationships in aquatic systems (Daufresne et al., 2009). In contrast to theoretical predictions, we observed an overall increase in size-at-age in most age classes due to density-dependent feedbacks (see Appendix D). Our study, together with results from Bassar et al. (2016), demonstrates that individuals do not necessarily get smaller under continuous warming, highlighting the importance of accounting for intrinsic dynamics in climate vulnerability assessments. Density-dependent growth appears to be a key mechanism for coping with climate changes or recovering from extreme climatic events (e.g., Bassar et al., 2016; Vincenzi et al., 2016). But in any case, the age-truncation effect can lead to unstable non-linear population dynamics that increase population fluctuations and thus the risk of collapse due to environmental stochasticity (Anderson et al., 2008). Human activities leading to disproportionally higher mortality of the largest individuals, like size-selective angling (Ayllón et al., 2018a), will amplify this problem.

The simulations also revealed that under the same climate projections, populations in more thermally challenging environments experienced lower survival, especially of age-2 and older trout, but exhibited stronger density-dependent, plastic and evolutionary responses. This explains why differences in rates of decline in abundance between populations under the warming-alone scenarios are not as large as one would expect, given that the main river has higher temperatures. Our simulations showed that reaches in the main river are not only more thermally challenging than the headwaters as temperature increases, but also more energy limited as flow decreases, due to their geomorphology: because our site in the main river is wider and shallower and has a U-type morphology, food availability decreases there at a higher rate than in the headwaters at very low flows. Letcher et al. (2015) also predicted that population responses to temperature variations are more flow-dependent in mainstems than in tributaries.

The critical role of hydrological change on trout persistence was further illustrated by the fact that the assumption that warming increases food production could not prevent extinction in either river type under the most extreme combined climatic scenario. This might initially be surprising, given the clear benefits of increasing food availability in both natural settings and in simulation models where fish can trade off food acquisition and predation risk (Railsback and Harvey, 2011). However, the increase in food production could not compensate for the effect of reductions in wetted area, water velocity and depth at extreme low flows, all of which reduce either the total amount of food produced or the ability of trout to capture food efficiently. Finally, our simplified food-change scenario linked food production only to temperature and not flow. Streamflow changes can alter food availability for drift-feeding fish in the short-term (Harvey et al., 2006; Naman et al., 2017), but long-term effects of altered streamflow regimes on food availability remain unclear.

Our simulations revealed many complex mechanisms affecting the trajectories of populations under shifting climates. Population trajectories were driven by the non-trivial responses of individual fish to changes both in their physical (space, thermal landscape, hydraulics) and biotic environment (patterns in food resources, levels of intraspecific competition). Forecasting the states of ecological systems is challenging and requires models as complex as necessary to realistically represent the study system (Evans et al., 2013; Ayllón et al., 2018b). Predictions from simple models that incorporate only a few relevant processes must be taken with caution. InSTREAM-Gen is structurally realistic and relatively complex, but of course its predictions are uncertain. One key issue is that prediction accuracy of our approach depends highly on the underlying feeding and bioenergetics models, which, as simplifications of complex behavioural and physiological processes, have substantial uncertainties of their own. These uncertainties include the structure and parameterization of the drift-foraging model, especially of the swimming cost and capture success functions (Rosenfeld et al., 2014); parameter uncertainty (Bartell et al., 1986); and the challenges of evaluating parameters at stressfully high temperatures (e.g., Myrick and Cech, 2000). Second, it is unclear how variability in temperature, flow or physical habitat influence invertebrate drift production and dynamics (Naman et al., 2016), or whether the energy content of prey will vary due to climate-driven shifts in community composition: future projections of food availability for trout are very uncertain. Third, we did not account for important indirect effects of climate change, particularly increased interactions (e.g., competition, predation, hybridization) with warm-water species, which might decrease population resilience. Warm-water species are rapidly expanding their altitudinal distribution and abundance in trout systems (e.g., Almodóvar et al., 2012) and temperature-dependent competition between salmonids and warm-water species has been documented (e.g., Reese and Harvey, 2002), but few studies link altered interactions between trout and warm-water fishes specifically to climate change (but see Muhlfeld et al., 2017). Those are critical research priorities to improve predictions of climate effects on trout populations.

5. Conclusions

Our simulations suggest that trout populations possess a variety of mechanisms that make them more resistant to global warming than previously thought. However, our simulations predict that warming leads to smaller populations consisting mainly of young individuals, which might be more unstable and prone to extinction if environmental variability increases, as it is expected to in Mediterranean freshwaters. Our study also predicts that concurrence of strong warming and flow reduction inevitably leads Mediterranean trout populations to extinction even if food production increases with temperature and even when we assume the possibility of rapid evolution in life history traits. Anthropogenic activities causing reduced flows, especially in summer, likely present a severe challenge to many trout populations in the coming decades.

Acknowledgements

Appendix A. Supplementary data

Supplementary data to this article can be found online at https://doi.org/10.1016/j.scitotenv.2019.133648.

References

Almodóvar, A., Nicola, G.G., Ayllón, D., Elvira, B., 2012. Global warming threatens the persistence of Mediterranean brown trout. Glob. Chang. Biol. 18, 1549–1560.

Anderson, C.N.K., Hsieh, C.H., Sandin, S.A., Hewitt, R., Hollowed, A., Beddington, J., May, R.M., Sugihara, G., 2008. Why fishing magnifies fluctuations in fish abundance. Nature 452, 835–839.

Ayllón, D., Almodóvar, A., Nicola, G.G., Elvira, B., 2010. Ontogenetic and spatial variations in brown trout habitat selection. Ecol. Freshw. Fish 19, 420–432.

Ayllón, D., Almodóvar, A., Nicola, G.G., Parra, I., Elvira, B., 2012. Modelling carrying capacity dynamics for the conservation and management of territorial salmonids. Fish. Res. 134-136, 95–103.

Ayllón, D., Nicola, G.G., Elvira, B., Parra, I., Almodóvar, A., 2013. Thermal carrying capacity for a thermally-sensitive species at the warmest edge of its range. PLoS One 8, e81354.

Ayllón, D., Railsback, S.F., Vincenzi, S., Groeneveld, J., Almodóvar, A., Grimm, V., 2016. InSTREAM-Gen: modelling eco-evolutionary dynamics of trout populations under anthropogenic environmental change. Ecol. Model. 326, 36–53.

Ayllón, D., Railsback, S.F., Almodóvar, A., Nicola, G.G., Vincenzi, S., Elvira, B., Grimm, V., 2018a. Eco-evolutionary responses to recreational fishing under different harvest regulations. Ecology and Evolution 8, 9600–9613.

Ayllón, D., Grimm, V., Attinger, S., Hauhs, M., Simmer, C., Vereecken, H., Lischeid, G., 2018b. Cross-disciplinary links in environmental systems science: current state and claimed needs identified in a meta-review of process models. Sci. Total Environ. 622-623, 954–973.

Bartell, S.M., Breck, J.M., Gardner, R.H., Brenkert, A.L., 1986. Individual parameter perturbation and error analysis of fish bioenergetics models. Can. J. Fish. Aquat. Sci. 43, 160–168.

Bassar, R.D., Letcher, B.H., Nislow, K.H., Whiteley, A.R., 2016. Changes in seasonal climate outpace compensatory density-dependence in eastern brook trout. Glob. Chang. Biol. 22, 577–593.

Bronaugh, D., Werner, A., 2015. zyp: Zhang + Yue-Pilon Trends Package. R Package Version 0.10–1.

Bruder, A., Salis, R.K., Jones, P.E., Matthaei, C.D., 2017. Biotic interactions modify multiple-stressor effects on juvenile brown trout in an experimental stream food web. Glob. Chang. Biol. 23, 3882–3894.

Comte, L., Grenouillet, G., 2013. Do stream fish track climate change? Assessing distribution shifts in recent decades. Ecography 36, 1236–1246.

Crozier, L.G., Hutchings, J.A., 2014. Plastic and evolutionary responses to climate change in fish. Evol. Appl. 7, 68–87.

Daufresne, M., Lengfellner, K., Sommer, U., 2009. Global warming benefits the small in aquatic ecosystems. Proc. Natl. Acad. Sci. U. S. A. 106, 12788–12793.

Eby, L.A., Helmy, O., Holsinger, L.M., Young, M.K., 2014. Evidence of climate-induced range contractions in bull trout Salvelinus confluentus in a Rocky Mountain watershed, U.S. A. PLoS One 9, e98812.

Eliason, E.J., Clark, T.D., Hague, M.J., Hanson, L.M., Gallagher, Z.S., Jeffries, K.M., Gale, M.K., Patterson, D.A., Hinch, S.G., Farrell, A.P., 2011. Differences in thermal tolerance among sockeye salmon populations. Science 332, 109–112.

Elliott, J.M., 1976. The energetics of feeding, metabolism and growth of brown trout (Salmo trutta L.) in relation to body weight, water temperature and ration size. J. Anim. Ecol. 45, 923–948.

Elliott, J.M., Elliott, J.A., 2010. Temperature requirements of Atlantic salmon Salmo salar, brown trout Salmo trutta and Arctic charr Salvelinus alpinus: predicting the effects of climate change. J. Fish Biol. 77, 1793–1817.

Evans, M.R., Bithell, M., Cornell, S.J., Dall, S.R.X., Díaz, S., Emmott, S., Ernande, B., Grimm, V., Hodgson, D.J., Lewis, S.L., Mace, G.M., Morecroft, M., Moustakas, A., Murphy, E., Newbold, T., Norris, K.J., Petchey, O., Smith, M., Travis, J.M.J., Benton, T.G., 2013. Predictive systems ecology. Proc. R. Soc. B Biol. Sci. 280.

Filipe, A.F., Markovic, D., Pletterbauer, F., Tisseuil, C., De Wever, A., Schmutz, S., Bonada, N., Freyhof, J., 2013. Forecasting fish distribution along stream networks: brown trout (Salmo trutta) in Europe. Divers. Distrib. 19, 1059–1071.

Foley, J.A., DeFries, R., Asner, G.P., Barford, C., Bonan, G., Carpenter, S.R., Chapin, F.S., Coe, M.T., Daily, G.C., Gibbs, H.K., Helkowski, J.H., Holloway, T., Howard, E.A., Kucharik, C.J., Monfreda, C., Patz, J.A., Prentice, I.C., Ramankutty, N., Snyder, P.K., 2005. Global consequences of land use. Science 309, 570–574.

Fullerton, A.H., Burke, B.J., Lawler, J.J., Torgersen, C.E., Ebersole, J.L., Leibowitz, S.G., 2017. Simulated juvenile salmon growth and phenology respond to altered thermal regimes and stream network shape. Ecosphere 8, e02052.

Grenouillet, G., Comte, L., 2014. Illuminating geographical patterns in species' range shifts. Glob. Chang. Biol. 20, 3080–3091.

Grimm, V., Berger, U., Bastiansen, F., Eliassen, S., Ginot, V., Giske, J., Goss-Custard, J., Grand, T., Heinz, S.K., Huse, G., Huth, A., Jepsen, J.U., Jorgensen, C., Mooij, W.M., Muller, B., Pe'er, G., Piou, C., Railsback, S.F., Robbins, A.M., Robbins, M.M., Rossmanith, E., Ruger, N., Strand, E., Souissi, S., Stillman, R.A., Vabo, R., Visser, U., DeAngelis, D.L.,

2006. A standard protocol for describing individual-based and agent-based models. Ecol. Model. 198, 115–126.

Grimm, V., Berger, U., DeAngelis, D.L., Polhill, J.G., Giske, J., Railsback, S.F., 2010. The ODD protocol a review and first update. Ecol. Model. 221, 2760–2768.

Harvey, B.C., Stewart, A.J., 1991. Fish size and habitat depth relationships in headwater streams. Oecologia 87, 336–342.

Harvey, B.C., Nakamoto, R.J., White, J.L., 2006. Reduced streamflow lowers dry-season growth of rainbow trout in a small stream. Trans. Am. Fish. Soc. 135, 998–1005.

Hodgens, L.S., Blumenshine, S.C., Bednarz, J.C., 2004. Great blue heron predation on stocked rainbow trout in an Arkansas tailwater fishery. N. Am. J. Fish Manag. 24, 63–75.

Isaak, D.J., Young, M.K., Nagel, D.E., Horan, D.L., Groce, M.C., 2015. The cold-water climate shield: delineating refugia for preserving salmonid fishes through the 21st century. Glob. Chang. Biol. 21, 2540–2553.

Isaak, D.J., Young, M.K., Luce, C.H., Hostetler, S.W., Wenger, S.J., Peterson, E.E., Ver Hoef, J.M., Groce, M.C., Horan, D.L., Nagel, D.E., 2016. Slow climate velocities of mountain streams portend their role as refugia for cold-water biodiversity. Proc. Natl. Acad. Sci. 113, 4374–4379.

Jonsson, B., Jonsson, N., 2011. Ecology of Atlantic Salmon and Brown Trout: Habitat as a Template for Life Histories. Springer, Dordrecht, Netherlands.

Kendall, M., 1975. Multivariate Analysis. Charles Griffin & Company, London.

Kennedy, R.J., Crozier, W.W., 2010. Evidence of changing migratory patterns of wild Atlantic salmon Salmo salar smolts in the River Bush, Northern Ireland, and possible associations with climate change. J. Fish Biol. 76, 1786–1805.

Kovach, R.P., Muhlfeld, C.C., Al-Chokhachy, R., Dunham, J.B., Letcher, B.H., Kershner, J.L., 2016. Impacts of climatic variation on trout: a global synthesis and path forward. Rev. Fish Biol. Fish. 26, 135–151.

Letcher, B.H., Schueller, P., Bassar, R.D., Nislow, K.H., Coombs, J.A., Sakrejda, K., Morrissey, M.B., Sigourney, D.B., Whiteley, A.R., O'Donnell, M.J., Dubreuil, T.L., 2015. Robust estimates of environmental effects on population vital rates: an integrated capture-recapture model of seasonal brook trout growth, survival and movement in a stream network. J. Anim. Ecol. 84, 337–352.

López-Moreno, J.I., Zabalza, J., Vicente-Serrano, S.M., Revuelto, J., Gilaberte, M., Azorin-Molina, C., Morán-Tejeda, E., García-Ruiz, J.M., Tague, C., 2014. Impact of climate and land use change on water availability and reservoir management: scenarios in the Upper Aragón River, Spanish Pyrenees. Sci. Total Environ. 493, 1222–1231.

Lynch, M., Walsh, J.B., 1998. Genetics and Analysis of Quantitative Traits. Sinauer Associates Inc., Sunderland, USA.

Mann, H.B., 1945. Nonparametric tests against trend. Econometrica 13, 245–259.

Milhous, R.T., Waddle, T.J., 2012. Physical Habitat Simulation (PHABSIM) Software for Windows (v.1.5.1). USGS Fort Collins Science Center, Fort Collins, CO.

Morin, A., 1997. Empirical models predicting population abundance and productivity in lotic systems. J. N. Am. Benthol. Soc. 16, 319–337.

Morin, A., Bourassa, N., 1992. Modèles empiriques de la production annuelle et du rapport P/B d'invertébrés benthiques d'eau courante. Can. J. Fish. Aquat. Sci. 49, 532–539.

Muhlfeld, C.C., Kovach, R.P., Al-Chokhachy, R., Amish, S.J., Kershner, J.L., Leary, R.F., Lowe, W.H., Luikart, G., Matson, P., Schmetterling, D.A., Shepard, B.B., Westley, P.A.H., Whited, D., Whiteley, A.R., Allendorf, F.W., 2017. Legacy introductions and climatic variation explain spatiotemporal patterns of invasive hybridization in a native trout. Glob. Chang. Biol. 23, 4663–4674.

Myrick, C. A., and J. J. Cech Jr. 2000. Temperature influences on California rainbow trout physiological performance. Fish Physiol. Biochem. 22:245–254.

Naman, S.M., Rosenfeld, J.S., Richardson, J.S., 2016. Causes and consequences of invertebrate drift in running waters: from individuals to populations and trophic fluxes. Can. J. Fish. Aquat. Sci. 73, 1292–1305.

Naman, S.M., Rosenfeld, J.S., Richardson, J.S., Way, J.L., 2017. Species traits and channel architecture mediate flow disturbance impacts on invertebrate drift. Freshw. Biol. 62, 340–355.

Palmer, M.A., Lettenmaier, D.P., Poff, N.L., Postel, S.L., Richter, B., Warner, R., 2009. Climatechange and river ecosystems: protection and adaptation options. Environ. Manag. 44, 1053–1068.

Parra, I., Nicola, G.G., Vøllestad, L.A., Elvira, B., Almodóvar, A., 2014. Latitude and altitude differentially shape life history trajectories between the sexes in non-anadromous brown trout. Evol. Ecol. 28, 707–720.

Railsback, S.F., Harvey, B.C., 2011. Importance of fish behaviour in modelling conservation problems: food limitation as an example. J. Fish Biol. 79, 1648–1662.

Railsback, S.F., Lamberson, R.H., Harvey, B.C., Duffy, W.E., 1999. Movement rules for individual-based models of stream fish. Ecol. Model. 123, 73–89.

Railsback, S.F., Harvey, B.C., Jackson, S.K., Lamberson, R.H., 2009. InSTREAM: The Individual-based Stream Trout Research and Environmental Assessment Model. U.S. Department of Agriculture, Forest Service, Pacific Southwest Research Station, Albany, CA.

Reese, C.D., Harvey, B.C., 2002. Temperature-dependent competition between juvenile steelhead and Sacramento pikeminnow. Trans. Am. Fish. Soc. 131, 599–606.

Ricker, W.E., 1975. Computation and interpretation of biological statistics of fish populations. Bulletin of the Fisheries Research Board of Canada 191, 1–382.

Rosenfeld, J.S., 2017. Developing flow-ecology relationships: implications of nonlinear biological responses for water management. Freshw. Biol. 62, 1305–1324.

Rosenfeld, J.S., Bouwes, N., Wall, C.E., Naman, S.M., 2014. Successes, failures, and opportunities in the practical application of drift-foraging models. Environ. Biol. Fish 97, 551–574.

Schewe, J., Heinke, J., Gerten, D., Haddeland, I., Arnell, N.W., Clark, D.B., Dankers, R., Eisner, S., Fekete, B.M., Colón-González, F.J., Gosling, S.N., Kim, H., Liu, X., Masaki, Y., Portmann, F.T., Satoh, Y., Stacke, T., Tang, Q., Wada, Y., Wisser, D., Albrecht, T., Frieler, K., Piontek, F., Warszawski, L., Kabat, P., 2014. Multimodel assessment of water scarcity under climate change. Proc. Natl. Acad. Sci. 111, 3245–3250.

Sundt-Hansen, L.E., Hedger, R.D., Ugedal, O., Diserud, O.H., Finstad, A.G., Sauterleute, J.F., Tøfte, L., Alfredsen, K., Forseth, T., 2018. Modelling climate change effects on Atlantic salmon: implications for mitigation in regulated rivers. Sci. Total Environ. 631-632, 1005–1017.

Taylor, K.E., Stouffer, R.J., Meehl, G.A., 2012. An overview of CMIP5 and the experiment design. Bull. Am. Meteorol. Soc. 93, 485–498.

Vincenzi, S., Mangel, M., Jesensek, D., Garza, J.C., Crivelli, A.J., 2016. Within- and among-population variation in vital rates and population dynamics in a variable environment. Ecol. Appl. 26, 2086–2102.

Wade, A.A., Hand, B.K., Kovach, R.P., Luikart, G., Whited, D.C., Muhlfeld, C.C., 2017. Accounting for adaptive capacity and uncertainty in assessments of species' climate-change vulnerability. Conserv. Biol. 31, 136–149.

Wenger, S.J., Isaak, D.J., Luce, C.H., Neville, H.M., Fausch, K.D., Dunham, J.B., Dauwalter, D.C., Young, M.I.K., Elsner, M.M., Rieman, B.E., Hamlet, A.F., Williams, J.E., 2011. Flow regime, temperature, and biotic interactions drive differential declines of trout species under climate change. Proc. Natl. Acad. Sci. U. S. A. 108, 14175–14180.

Yue, S., Pilon, P., Phinney, B., Cavadias, G., 2002. The influence of autocorrelation on the ability to detect trend in hydrological series. Hydrol. Process. 16, 1807–1829.